

A STUDY ON TRANSIENT WEAR BEHAVIOR OF NEW FREIGHT WHEEL PROFILES DUE TO TWO POINTS CONTACT IN CURVE NEGOTIATION

MORAD SHADFAR, HABIBOLLAH MOLATEFI

School of Railway Engineering, Iran University of Science and Technology, Tehran, Iran
e-mail: morad.shadfar@gmail.com; molatefi@iust.ac.ir

Systematic examinations on wear behavior of stick/slip contact around metal on metal have shown that the dissipated energy and contact forces are two important parameters of wear of wheels and rails. Nevertheless, an accurate estimation of these parameters is still a great challenge. Recent developments of non-linear dynamical models and simulation of operational conditions have tried to find a solution of this challenge. These results are used as the input to calculations of wear propagation. Though, the dynamic model should be able to predict wheel-rail interaction with high accuracy. In addition, wheel-rail wear is a function of several other parameters whose their integrated influence becomes more than the main discussed ones. In this study, with the help of multi-body dynamics (MBD), an open wagon equipped with three pieces bogies, considering non-linear effects of friction wedges and structural clearances is modeled in Universal Mechanism. Tangent and curved sections of the track considering random vertical and lateral irregularities are simulated. The simulation results are used to calculate wear of both left and right wheels separately. Specht's wear model based on Archard's wear model is used. The studied parameters are the rail side coefficient of friction, track quality, track curvature, velocity and rail side wear. Finally, the effects of mentioned parameters are studied on wear depth and wear pattern of new wheel profiles under incompatible contact (which occurs in Iran railway network). The results show different wear volume and wear pattern compared to compatible contact.

Keywords: three pieces bogie, Specht wear theory, wear depth, incompatible contact, rail side wear

1. Introduction

Scientific investigations on the rolling contact problem were begun in early of the 20'th century. The primary results showed the dependency of motion state on the wheel-rail contact forces. A practical progress was made in the late sixties and early seventies. In 1967, the computer based theory of Kalker was known by railway experts and as a consequence, this theory found practical applications in railway industries.

The first investigation on wear of railway wheel profiles was based on computer simulations with simple and steady state considerations, like constant velocity on ideal tangent track (Zobory, 1997). Sherrat and Pearce (1991) presented a very simple model. In their model after calculation of contact forces and creepages, the volume of removal mass was calculated with a wear index. They also considered one S track followed by a tangent track (Braghin *et al.*, 2006). In some works, there is an emphasis on the relation between the maximum contact pressure and removal mass which sometimes considered coefficients as the effects of energy (Zobory, 1997; Telliskiv and Olofsson, 2004). Nevertheless, most assumptions in wear are used in the correspondence of dissipated energy in the slip area and special removed mass per unit distance ([5], Jendel, 2002; Enblom and Berg, 2005; Pombo *et al.*, 2011; Jin *et al.*, 2011; [13]).

Most of the researchers consider that the wear phenomenon occurs only in the wheel, not in the rail. Also in the models, a linear relation between wear and friction work is usually assumed

(Zakharov and Zharov, 2002). Examination of changes in the contact point could lead to predict catastrophic wear which has great importance for increasing velocity (Telliskiv and Olofsson, 2004). Zobory used two different wear regimes: mild wear on the wheel tread and severe wear in the flange (Braghin *et al.*, 2006).

Recent investigations give us an ability to predict wear of the wheel-rail system under specified operation with reasonable accuracy. As a consequence, one can model tangent and curve sections of the track and simulate passage frequency in numerical analysis of railway operation. This process could be done on tracks with random irregularities. With the help of simulation results, the wear volume of the rail and wheel can be calculated on different sections of the track. It is common to use contact codes like CONTACT, FASTSIM or other innovative codes in such works (Braghin *et al.*, 2006). For example, Iwnicki and Xie (2008) considered a 3D wheel-rail system for calculation of the rail head wear in the presence of short pitch irregularity, considering non-Hertzian and non-steady contact based on Kalker's method (Xie and Iwnicki, 2008a,b).

In this study, with the use of a 3D non-linear dynamic model in the presence of random irregularities, sensitivity analysis of the wear pattern for different parameters is performed. The innovation in this paper is the examination of wear in presence of two point contact due to incompatible contact. As it is seen later, the effects of operational parameters would be different compared to compatible, one point contact.

2. Iran railway network

Iran geographic location in the Middle East caused freight mass transit development in comparison to passenger transporting. In the recent years, with respect to an increase in the transit volume and vehicle ages, variant wheel defects are reported by National Railway Administration [1]. These defects are different from one vehicle type and age to another, but most of the wheels show 1 mm hollow tread at early passages.

Although wheels show little hollow tread on early service life, but these hollows do not fall into repair regulations. With the use of these wheels in service, finally thin flanges would cause the wheels to reject. By considering harmful effects of the hollow tread especially in lubricated curves [5], there is a necessity for a comprehensive study around dynamic performance and energy consumption of vehicles. Figure 1 shows a 1 mm hollow tread after 10 000 km passage. Table 1 shows total repaired wheel defects in a range of 14 months [1].



Fig. 1. Tread defects after 10 000 km passage

Table 1. Total repaired wheel defects (April 2010 – June 2011) [1]

Defect type	No. of recorded wheels
Hollow tread	104
Un-conical wheel	58
Sharp flange	847
Thin flange	2085
Total wheel defects	5612

3. Wear

According to Zakharov’s theory, wear of the wheel and rail are generally proportional to the energy used to overcome the rolling resistance of the wheels and rails [5]. Wear of the wheels and rails is defined with the stress P and relative slip in contact area. Wear is also dependent on the third layer properties which depend, in turn, on lubrication, environment conditions and sand. On the basis of laboratory tests under un-lubricated conditions, three different wear regimes are defined: mild, severe and catastrophic. Figure 2 shows a shakedown diagram. It determines areas of normal and un-normal performance. P is the maximum contact pressure and λ is creepage. The curve $P\lambda = 40$ determines changes in the wear regime from mild to severe while $P\lambda = 120$ is the change between severe to catastrophic wear [5].

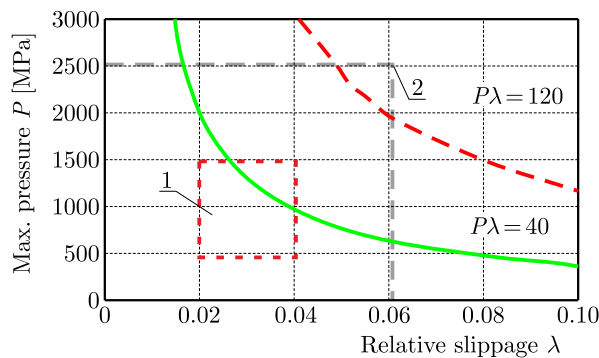


Fig. 2. Shakedown diagram for steel wheels and rails: normal area (1) and abnormal area (2)

3.1. Mathematical description of wear

For mild and severe modes of wear, the wear rate can be defined as a linear function of friction work [5]. The friction work can be defined as

$$A = \int_0^t v(t)(F_x \zeta_x + F_y \zeta_y) dt \tag{3.1}$$

where A is the friction work, v stands for velocity, F_x and F_y are longitudinal and lateral contact forces, and ζ_x and ζ_y are creepages which are defined

$$\xi = \frac{r\omega - \mathbf{V}}{\mathbf{V}} \tag{3.2}$$

where r is wheel radius and ω is angular velocity of the wheel. All dimensions are in SI.

One of the most applicable wear theories was presented by Archard (Jendel, 2002). He considered a linear relation between the wear volume and friction work. Accordingly

$$I = K_v A \tag{3.3}$$

where I is in m^3 and K_v is the wear volume coefficient [m^3/J].

For the use of this model, it is necessary to determine the coefficient K_v at any instance. Specht suggested a jumping factor α for every wear regime, therefore K_v can be assumed constant. By implementing the jumping factor into Archard’s equation, it can be rewritten as follows

$$I = \begin{cases} K_v A & \text{for } w < w_{cr} \\ K_v \alpha A & \text{for } w \geq w_{cr} \end{cases} \tag{3.4}$$

where w is the friction power [s/m^2] (friction work per second per contact area) and w_{cr} is the critical friction power which defines the wear regime and changing condition from mild to severe. Equation (3.4) is known as Specht wear model [13].

3.2. Determination of the wear coefficient

Several experiments for determining the coefficient K_v has been performed. As a result, a step change in the wear coefficient was obtained by deferent researchers.

The magnitude of K_v has a dependency in the wheel-rail material and its mechanical property. A typical magnitude for common wheels and rail is $10^{-13} \text{ m}^3/\text{J}$ and 10 for the jumping factor. By consideration of a mild wear amplitude, it can be reasonable to assume that the most part of the removed mass in the railway is due to the severe wear mode.

3.3. Wear calculation algorithm

For calculation of wear of the wheel and rail and its pattern, a sophisticated dynamic model is required. So it is possible to determine accurately shear forces and creepages in contact area at any instance. Zobory with the help of Medyna software calculated wear of wheels and rails in a specific track. The results showed a 5% difference compared to the final field test. The reason was neglecting the effects of switches. Lewis and Olofsson (2009) calculated wear of wheels with ADAMS/RAIL. Similar works were performed by Malvezzi with the help of Simpack and MATLAB and Pombo by Vampire software. In spite of differences in the software, all the works followed the same algorithm presented in Fig. 3. Global parameters contain contact forces, points, area, creepages calculated in time domain and imported into wear calculation. With the use of the wear model wear, depth at any point is calculated, the wheel and rail profile is updated and analysis continued to the next iteration. In this paper, Universal Mechanism software is used for both dynamic and wear modeling.

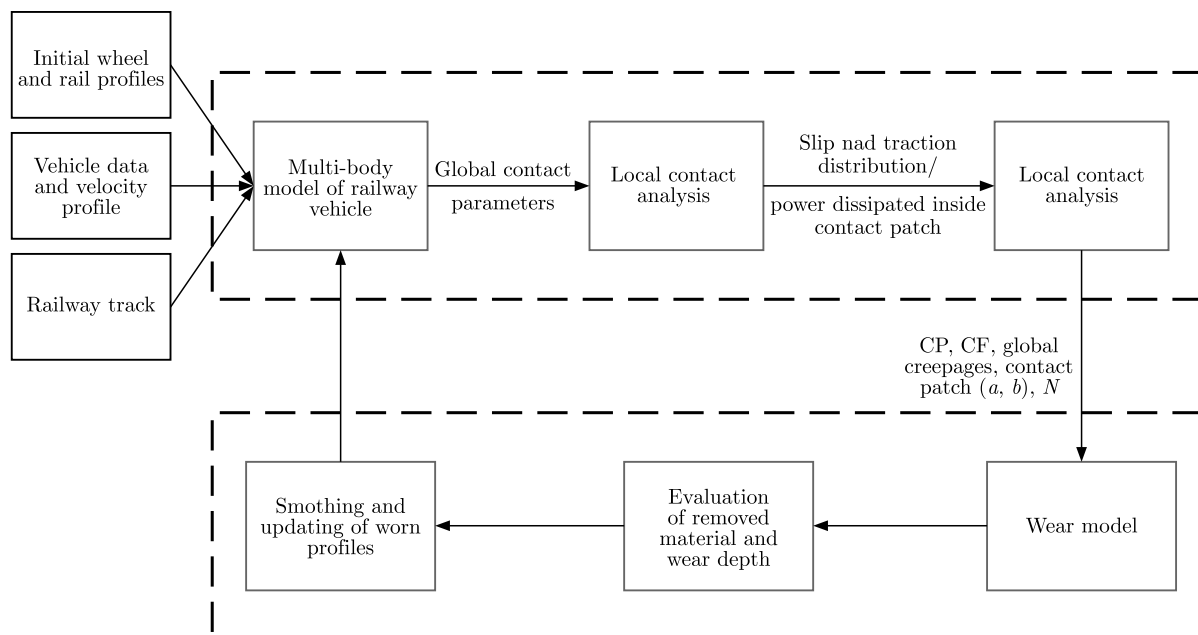


Fig. 3. Wear algorithm

4. Dynamic model requirements for the train-track system

The process of wheel-rail wear simulation always needs a proper dynamic environment which is able to make an access to real load and motion data (that show the operation conditions of the train-track system) for analysis of the removed mass. This dynamic model can be defined in deferent levels of detail but it should be able to calculate contact forces and creepages with a high accuracy.

4.1. Three pieces bogie

Three pieces bogies have been used in deferent railway networks for more than 60 years. In Iran, Russian bogies are widely used in mass transportation. Iran railway equipped 7100 wagons with these bogies [1]. Table 2 shows types and number of Iran railway wagons equipped with 18100 bogie.

Table 2. Iran wagons equipped with 18100 bogies [1]

Wagon type	Number of wagons
Low-sided wagon	1653
Open wagon	3716
Flat wagon	231
Tank car	461
Hooper ballast wagon	200
Hooper wagon	746

These bogies use S1002 wheel profile running on the rail UIC60 with rail inclination 1:20 which leads to two point contact as it is shown in the results. This wheel-rail arrangement is not suggested in the standard operation [11]. This arrangement results in improper steering and severe wear during curve negotiation. It also applies different wear pattern for both the wheel and rail. In such conditions, effects of parameters like rail side lubrication, velocity and track quality could be different.

A typical three pieces bogie consists of two side frames which are attached each other with the help of secondary suspension system and a bolster. Damping is provided with 4 friction wedges which move in vertical and lateral directions.

The wheels with the use of adapters are directly connected to side frames (Fig. 4). The friction force between adapters and side frames are modeled considering clearances in the UM template. Direct connection between the adapters and side frames results in high un-sprung mass and high dynamic loads. Low adapter clearances in both vertical and lateral directions lead to high bending and shear stiffness of the bogie. This causes imperfect curving of the wheels.

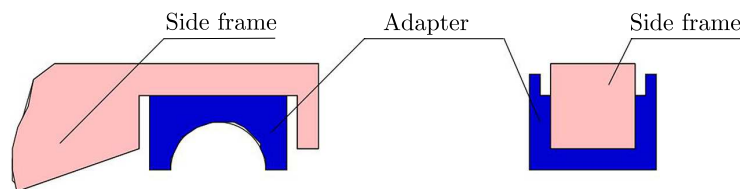


Fig. 4. Connection between an adapter and a side frame

A very unique phenomenon in the three pieces bogie is warping. It usually happens in curves and also some defects like hollow tread could intensify that. As a consequence of warping, high angle of attack and flange contact in both left and right wheels occurs. This results in flange wear

in both left and right wheels simultaneously. Warping makes 18100 bogie unfair for non-straight corridors. Figure 5 shows a schematic warping of the three pieces bogie.

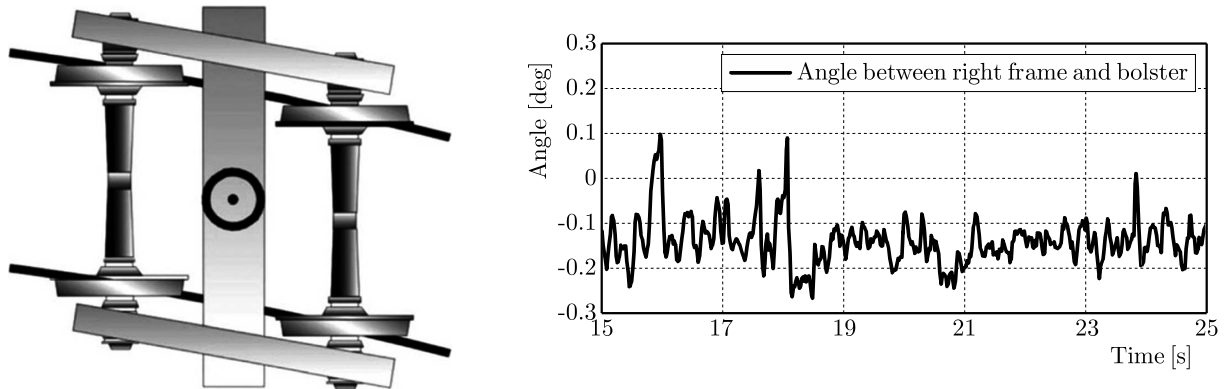


Fig. 5. Warping of the three pieces bogie

Two dimensional wedges let the bolster to damp vibrations in both vertical and lateral directions but implement nonlinearity into the model. Pivot friction and side bearers are also considered in the UM template. Tables 3 to 5 describe parameters of the three pieces bogie which is available in Universal Mechanism software.

Table 3. Inertial parameters of the train

Part	Mass [kg]	CG [m] (from rail surface)	I_{xx} [kg·m ²]	I_{yy} [kg·m ²]	I_{zz} [kg·m ²]
Wheelset	1500	0.475	925	200	925
Axle box	11	0.475	0.04	0.157	0.16
Side frame	526.3	0.525	13.96	175.8	161.8
Bolster	682.6	0.649351	412.609	11.06	415.909
Carbody	90000	1.4	21840	53919	66800

Table 4. Parameters of the suspension system

Part	K_x [N/m]	K_y [N/m]	K_z [N/m]	K_t [Nm/rad]	Coefficient of friction
Secondary suspension	8 · 643000	8 · 643000	8 · 632000	8 · 3325000	–
Wedges	710000	100000	2 · 632000	–	0.3

Table 5. Wheelset parameters

Wheel bases space [m]	1.85
Tap circle distance [m]	1.5
Longitudinal clearance [mm]	5
Lateral clearance [mm]	5
Wheel profile	S1002

In order to verify the model, non-linear hunting velocity of the bogie is extracted. This velocity is calculated about 95 km/h (26.3 m/s). In the next step, vertical acceleration of the model is compared with the field test mentioned in (Hosein Nia, 2011). The track consists of a tangent track followed by a curve.

Figure 6 shows vertical acceleration of the measured data and simulated one. The measured acceleration is in the range of $\pm 0.5 \text{ m/s}^2$ and, the MBD model shows a good agreement in both frequency and amplitude.

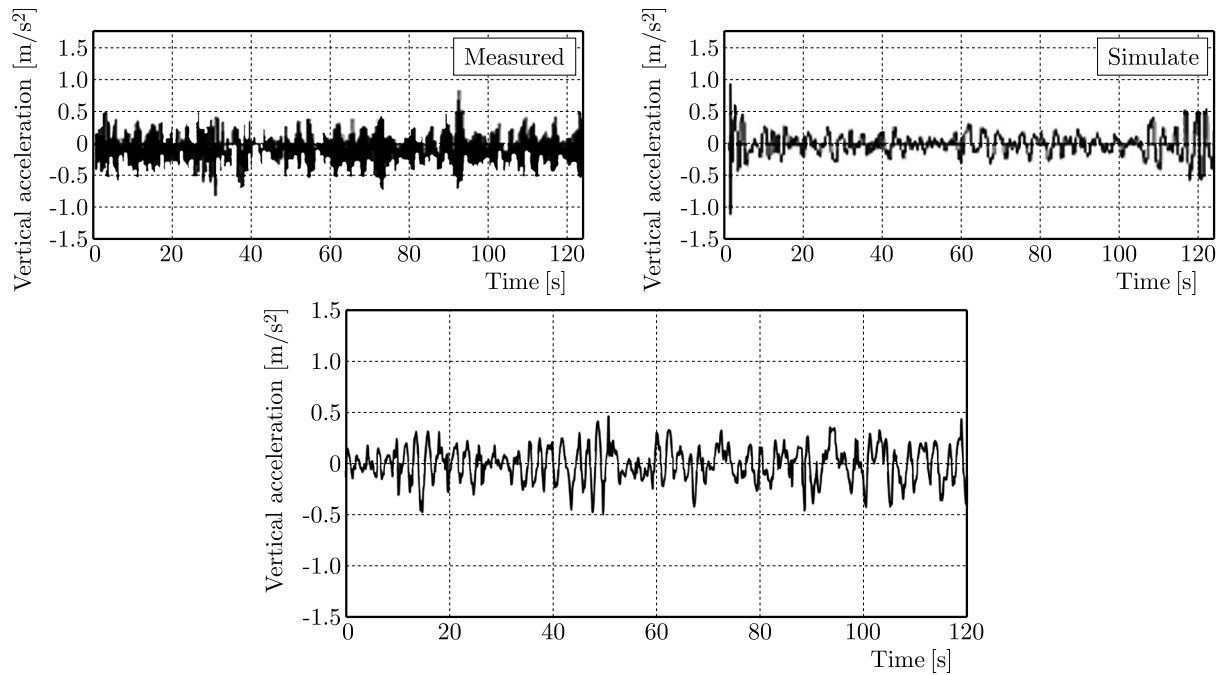


Fig. 6. Comparison between the measured and simulated vertical acceleration (Hosein Nia, 2011) (up) and simulated model in UM (down)

5. Analysis assumptions

This part includes wear analysis results by running a train on different tracks and rail profiles. The parameters are rail-side coefficient of friction, velocity, track curvature and quality. Table 6 describes the change in each parameter. These analyses are performed for each rail profile.

Table 6. Studied range for parameters

Case number	Cant [mm]	Radius of curvature [m]	Velocity [m/s]	Rail side coefficient of friction	Class (FRA)
1	150	600	25	0.1	3
2	150	600	25	0.2	3
3	150	600	25	0.3	3
4	100	500	25	0.2	3
5	100	700	25	0.2	3
6	100	1000	25	0.2	3
7	150	600	25	0.2	3
8	150	600	25	0.2	6
9	100	600	16	0.2	3
10	100	600	20	0.2	3
11	100	600	25	0.2	3

The rail profiles are considered in four different forms as it shown in Fig. 7. The rail profiles are called new profile, worn 1, worn 2 and worn 3, where worn 1 has the least and worn 3 has the most side wear. It should be noted that high and low rails have different profiles in their

worn shapes. All the wheel profiles are considered to be new at the beginning of analysis. The rail profiles are also considered to be constant in the whole track.

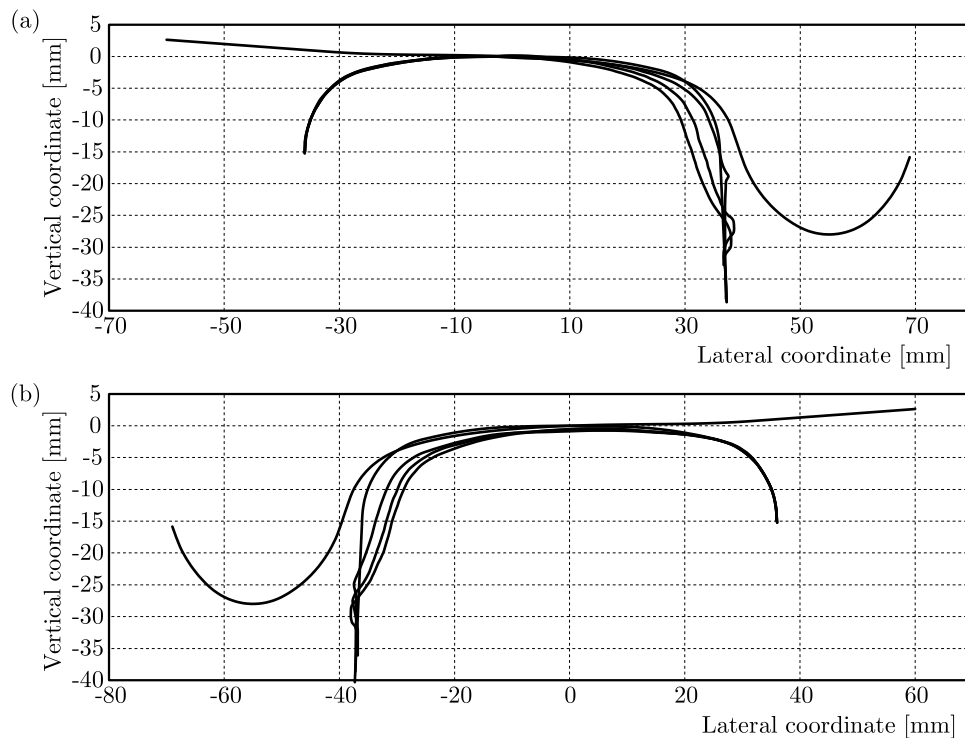


Fig. 7. Worn rail profiles (Lewis and Olofsson, 2009): high rail (left) and low rail (right)

The simulated train consists of 4 wagons as a typical example of a complete train including locomotive, first wagon, middle wagons and the last wagon. The results are gathered from wagon 3 as it is shown in Fig. 8.

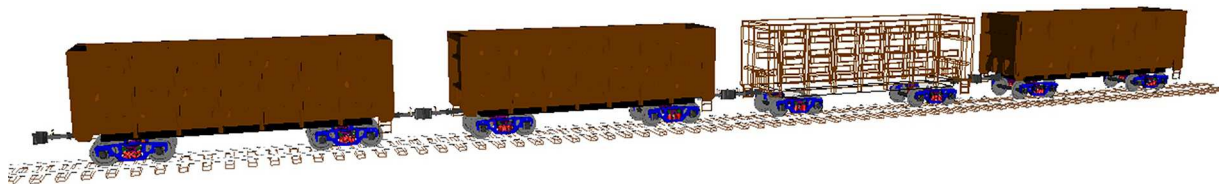


Fig. 8. Simulated 3D train

The train passes over a track and the results are saved at every passage. The track consists of a 40 m tangent track, 130 m spiral, 500 m curve section and the final 130 m spiral.

This analysis is done 15 times.

6. Results

Figure 9 shows rolling radius difference (RRD) against lateral displacement of the wheel. The rail profile is UIC 60 and rail inclinations of 1:20 and 1:40, and the wheel profile is S1002. In the rail inclination 1:40, there is a rolling difference for every lateral displacement. So, for each lateral displacement, there is a different point on the wheel. This causes uniform wear along the wheel profile and prevents local wear like hollow tread. In contrast to 1:40, in 1:20 inclination, there is no significant distribution and the contact point remains constant at the first 6 mm of

wheel lateral displacement. As a result, for each curve, the wheel has to make a flange contact, so high flange wear occurs.

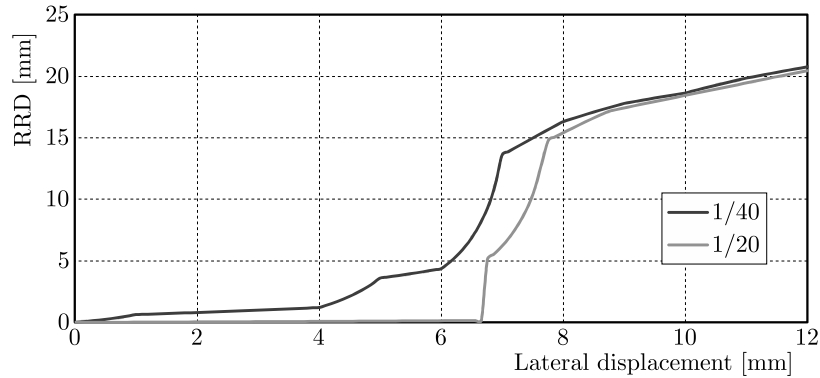


Fig. 9. Effects of rail inclination on rolling radius difference (RRD) in right and left wheels

6.1. Wheel-rail compatibility

Figure 10 (left) shows all possible contact points between the wheel and rail. From the top to down side, wear of the rail profiles increases. For a new rail (up) there are two discrete contact zones. So, local wear in this arrangement is expected. With an increase in rail wear, these two zones merge together in order to make a united zone, so a more uniform rate of the contact point change occurs.

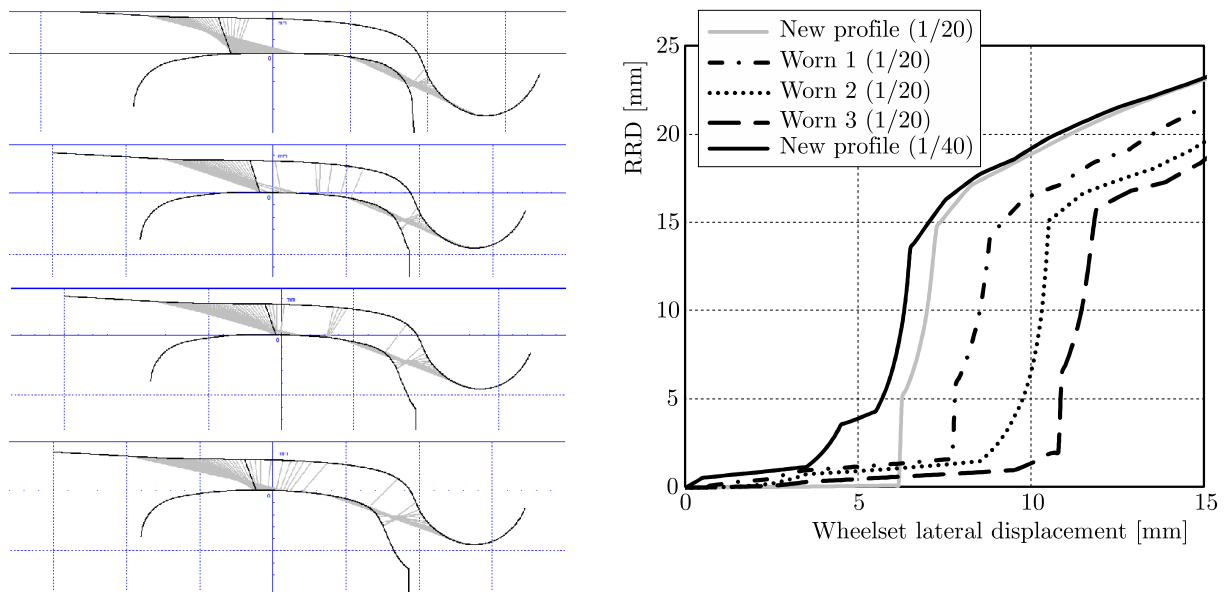


Fig. 10. Contacts for each profile pair (new wheel and worn rails) (left) and RRD diagrams for each profile pair (right)

Figure 10 (right) shows an RRD diagram for profile pairs in Fig. 10 (left). It also includes new wheel and rail profiles in the standard arrangement (rail inclination 1:40). If 1:40, the diagram is considered as standard dynamic performance, so the wear pattern tends to move toward standard at worn rail 1. But with an increase in the rail-side wear and material loss, this dynamic performance descends. So, as a very important result in this part, in an incompatible or non-standard arrangement the wear pattern tends to move towards the standard performance,

but this balance will never get completed. With an increase in the material loss, the dynamic performance becomes much like a non-standard one again.

The analysis is performed and wear depth for each scenario is calculated. Figure 11 shows wear depth of the outer wheels. The wear pattern and wear amplitude in two bogies were the same, so only the outer wheels of the front bogie is plotted. As it is expected, wear of the wheels in contact with the new rail is more than the worn ones. In ideal, the wear pattern and depth of all wheels should be the same, so more differences in the wear pattern and more imperfect curving behavior could be concluded. In Fig. 11, the leading wheels experience flange wear while the trailing wheels tend to have tread wear. The trailing wheel with the new rail profile shows flange wear, too. The reason is sharp negative angle of attack and this, as it is shown in Fig. 11, is eliminated with an increase in the wheel-rail clearance (increase in rail side wear). The train passes over a simple curve, so discrete flange and treads wear shows two points contact. This phenomenon due to the incompatible arrangement happens in all cases. Discrete wear of 18100 wheels and hollow tread of new wheel profiles are discussed in Section 2. Kalousek (2005) also reported discrete wear of 18100 wheel profiles.

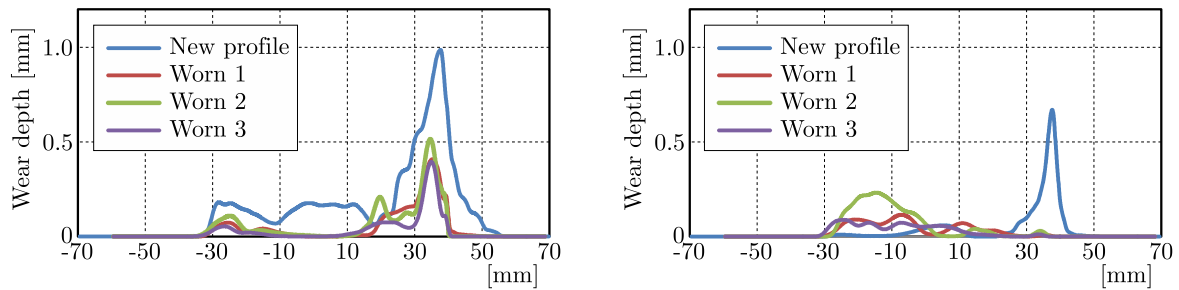


Fig. 11. Wear depth diagram for the outer wheels of the front bogie, leading wheel (left) and trailing wheel (right). Rail-side coefficient of friction is 0.1

Figure 12 shows a change in the RRD diagram of worn wheel profiles compared to the new one. For all rail profiles (new, worn 1 to 3), wheel wear approaches the standard mode. This change is negligible for the new rail but worn rail 1 exhibits biggest change in dynamic behavior. As it was mentioned before, RRD changes from worn rail 1 to 3 decrease because of too much material loss and the loss of system balance.

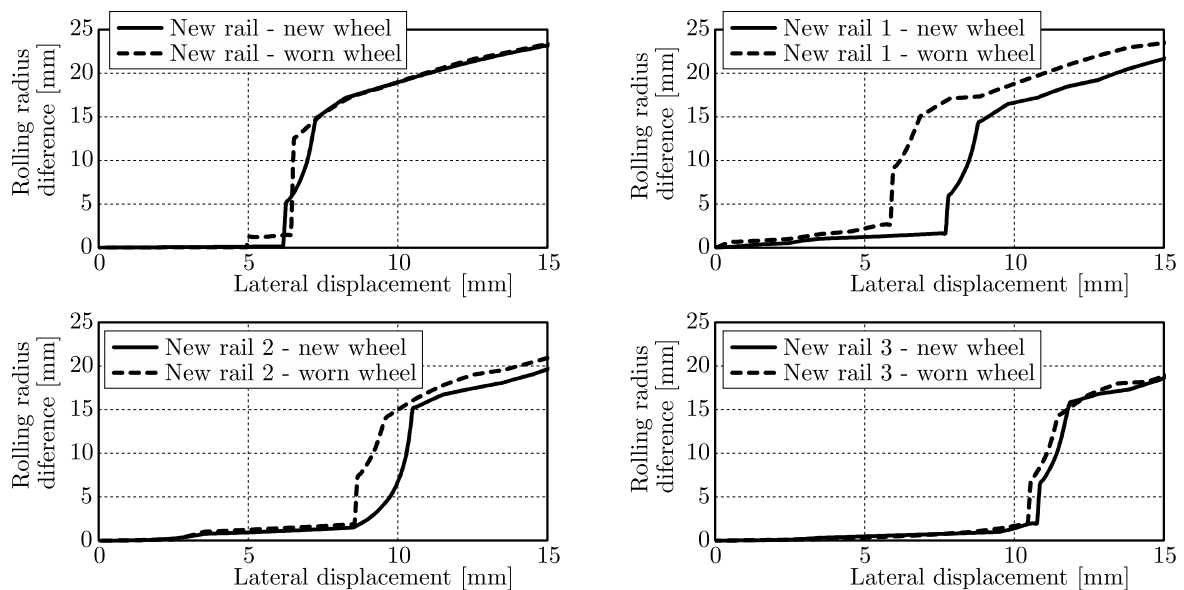


Fig. 12. Comparison of RRD diagrams for worn and new wheel profiles

6.2. Effect of operational parameters

6.2.1. Effect of rail-side friction

With a decrease in rail-side lubrication, the total friction work reduces, but too much reduction will cause an increase of the work in new rail profile. The reason is the harmful effect in bogie steering and creepages which decrease significantly. Figure 13 shows a comparison between wear depth for rail inclinations 1:20 and 1:40. The wear pattern becomes continuous along the wheel profile. The reason is the one point contact which results in a continuous and smooth change in the contact point. A change in the rail side coefficient of friction results in a very clear pattern of wear of the wheels. On the other side (incompatible wheel-rail arrangement), wear depth is discrete due to two point contact and a sudden change in the contact point from tread to flange. In contrast to 1:40 ones, the change in the coefficient of friction results in a no clear pattern. The wear depth amplitude increases in unfair arrangement and it can be concluded that two the point contact reduced the efficiency of rail side lubrication. From the results for both 1:40 and 1:20 inclinations, wear depth of 0.8-1.0 mm in only 12 km curve passage is not economical. This determines that the three pieces bogie is not suitable for non-straight corridors.

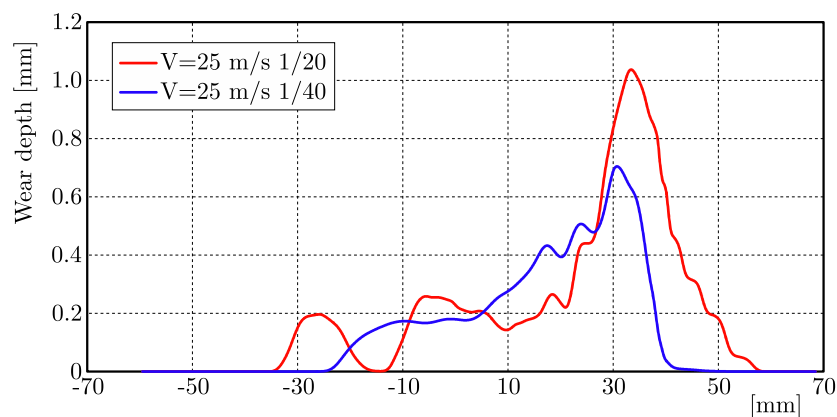


Fig. 13. Comparison of wear depth for the leading wheel (1:20 and 1:40 rail inclination and a new rail profile)

6.2.2. Effect of track quality

The change in the track class results in a very clear pattern in wheels though the irregularities are random (Fig. 14). In the new rail profile, wear decreases with an increment of track quality. But this pattern is changed in worn rails. The leading wheel shows more wear in class 6 but the trailing wheels have less wear when compare to class 3. Imperfect curving is still the key parameter for non-uniform wear of the wheels. Also two the point contact can be concluded from the diagrams.

Figure 15 shows the total friction work during analysis. On the basis of this diagram, track quality has a noticeable effect on the rolling resistance of the wheels and, consequently, noticeable effect on energy consumption of the vehicles.

6.2.3. Effect of velocity

Velocity is the most important parameter in wear. Figure 16 shows wear depth of the wheel profile passing over a new rail. Wheel tread is more sensible to a change in velocity. With an increase in speed, the leading wheels have less wear in their tread while the trailing ones experience more. On the other hand, an increase in velocity results in better steering and more uniform wear in all wheels.

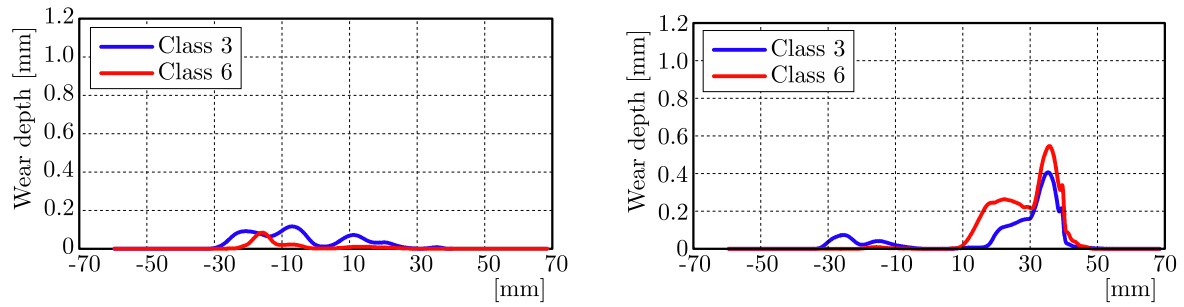


Fig. 14. Wear depth diagram for the outer wheels of the front bogie, leading wheel (left) and trailing wheel (right) (worn rail No. 1)

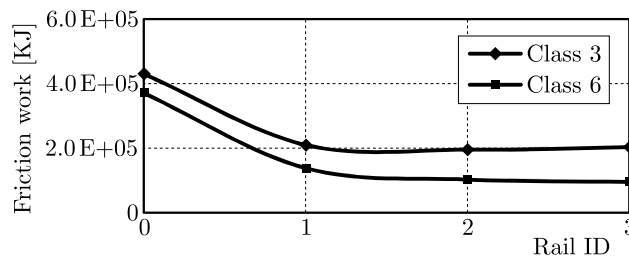


Fig. 15. Friction work for different rail profiles and track quality

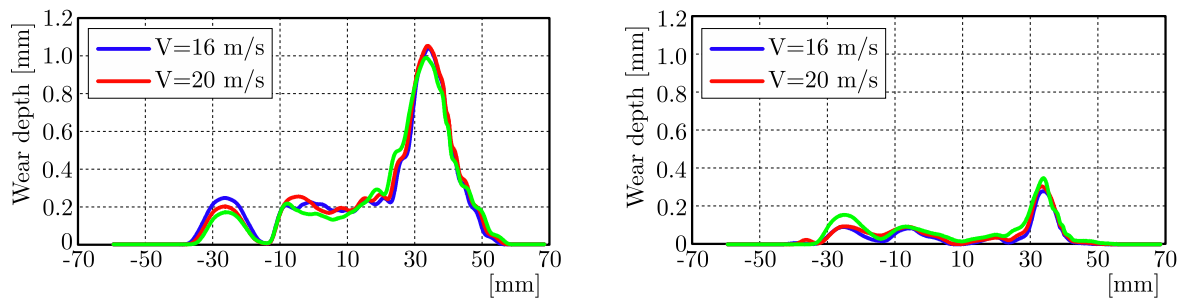


Fig. 16. Wear depth diagram for the outer wheels of the front bogie, leading wheel (left) and trailing wheel (right) (new rail profile)

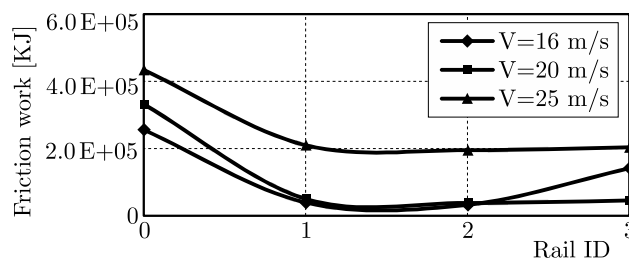


Fig. 17. Friction work for different rail profiles and velocities

Figure 17 also shows the total friction work during analysis. With an increase in speed, the friction work increases while in the wear depth, volume of the removed mass is not changed noticeably. The reason is better steering of bogies, so the bogie spends shorter time in the severe wear mode. All worn rails show a lower friction work compared to the new rail profile as it is expected.

7. Conclusion

In this study, the effect of rail side wear on the wear pattern of new wheel profiles is examined. The parameters are the rail side coefficient of friction, track quality, track curvature and velocity. With respect to the analysis conditions, the effects of wheel-rail clearance and curving behavior of a selected bogie (pivot friction) are taken into account.

The results show that imperfect curving of the bogie is the key parameter for non-uniform wear of wheels. Non-uniform wear may result from the tangential force. The wheel-rail clearance also has great influence in the new wheel wear pattern. The results can be summarized as follows:

- Contact analysis of new wheel profiles with different worn rails show discrete contact zones along new wheel and new rail profiles. These zones are merged with an increase in the rail wear.
- The wear pattern of new wheels approaches the standard mode. The change in an RRD diagram is the most for worn rail 1 and descends to worn rail 3.
- Rail-side lubrication is a common way for reducing lateral forces. But the two point contact could easily undo the advantages of lubrication.
- The track class has a very clear effect on the wheels, though the irregularities are random. In the new rail profile, wear decreases with an increase in track quality.
- Track curvature effects become eliminated by the increase in the wheel-rail clearance. This parameter needs more detailed investigation.
- Velocity has the most effect on the wear pattern for new wheel profiles.
- The importance of compatible contact becomes high for changing velocity conditions.
- With an increase in velocity under incompatible contact, wear of wheels becomes more uniform.

Based on the results, Iran Railway Research Center organized a field test for calibrations of the results in wear depth. The wheel and rail wear will be monitored the during following year, and the results will be used in order to optimize the wheel-rail contact quality.

References

1. Archives of the National Railway Organization of I.R.Iran, Freight Wagons Division
2. BRAGHIN F., LEWIS R., DWYER-JOYCE R.S., BRUNI S., 2006, A mathematical model to predict railway wheel profile evolution due to wear, *Wear*, **261**, 1253-1264
3. ENBLOM R., BERG M., 2005, Simulation of railway wheel profile development due to wear-influence of disc braking and contact environment, *Wear*, **258**, 1055-1063
4. HOSEIN NIA S., 2011, *Dynamics Modeling of Freight Wagons*, Master's Degree Thesis, Department of Mechanical Engineering, Blekinge Institute of Technology, Karlskrona, Sweden
5. International Heavy Haul Association (2001), *Guidelines to best practices for heavy haul railway operations: wheel and rail interface issues*, 2808 Forest Hills Court Virginia Beach, Virginia 23454 USA
6. JENDEL T., 2002, Prediction of wheel profile wear-comparisons with field measurements, *Wear*, **253**, 89-99
7. JIN Y., ISHIDA M., NAMURA A., 2011, Experimental simulation and prediction of wear of wheel flange and rail gauge corner, *Wear*, **271**, 259-267
8. KALOUSEK J., 2005, Wheel/rail damage and its relationship to track curvature, *Wear*, **258**, 1330-1335

9. LEWIS R., OLOFSSON U., 2009, *Wheel-Rail Interface Handbook*, CRC Press, Boca Raton, Boston, New York, Washington, DC
10. POMBO J., AMBROSIO J., PEREIRA M., LEWIS R., DWYER-JOYCE R., ARIAUDO C., KUKA N., 2011, Development of a wear prediction tool for steel railway wheels using three alternative wear functions, *Wear*, **271**, 238-245
11. Rail Safety and Standards Board (2002), *Feasibility of reducing the number of standard wheel profile designs*, Report No. ITLR/T11299/001
12. TELLISKIVI T., OLOFSSON U., 2004, Wheel/rail wear simulation, *Wear*, **257**, 1145-1153
13. Universal Mechanism User's Manual (2012), *Railway wheel and rail profile wear prediction module*, UM Laboratory
14. XIE G., IWNICKI S.D., 2008a, Calculation of wear on a corrugated rail using a three-dimensional contact model, *Wear*, **265**, 1238-1248
15. XIE G., IWNICKI S.D., 2008b, Simulation of wear on a rough rail using a time-domain wheel-track interaction model, *Wear*, **265**, 11/12, 1572-1583
16. ZAKHAROV S., ZHAROV I., 2002, Simulation of mutual wheel/rail wear, *Wear*, **253**, 100-106
17. ZOBORY I., 1997, Prediction of wheel/rail profile wear, *Vehicle System Dynamics*, **28**, 221-259

Manuscript received July 29, 2014; accepted for print December 16, 2016